Published in final edited form as:
Anat Rec (Hoboken). 2013 December ; 296(12): 1821–1832. doi:10.1002/ar.22822.

Mediation of muscular control of rhinarial motility in rats by the nasal cartilaginous skeleton

Sebastian Haidarliu[1,*], **David Kleinfeld**[2], and **Ehud Ahissar**[1]

[1]Department of Neurobiology, The Weizmann Institute of Science, Rehovot, Israel.

[2]Department of Physics and Section of Neurobiology, University of California at San Diego, La Jolla, CA 92093, USA.

Abstract

The *Rhinarium* is the rostral-most area of the snout that surrounds the nostrils, and is hairless in most mammals. In rodents, it participates in coordinated behaviors, active tactile sensing, and active olfactory sensing. In rats, the *Rhinarium* is firmly connected to the nasal cartilages, and its motility is determined by movements of the rostral end of the nasal cartilaginous skeleton. Here we demonstrate the nature of different cartilaginous regions that form the *Rhinarium* and the nasofacial muscles that deform these regions during movements of the nasal cartilaginous skeleton. These muscles, together with the dorsal nasal cartilage that was described here, function as a rhinarial motor plant.

Keywords

nasofacilal muscles; rhinarium; rodents; vibrissa; whisking

INTRODUCTION

In rodents, rostral structures of the face are mobile and participate in active tactile and olfactory sensing. These structures include sensory hairs, such as macrovibrissae and microvibrissae (Brecht et al., 1997), and the *Rhinarium* with its prominent narial pads (Hill, 1948; Ade, 1999), or nasal tubercles (Smith and Monie, 1969). The morphology and innervation of the *Rhinarium* have been described in detail in several species, *i.e.*, coati and raccoon (Barker and Welker, 1969), opossum (Pubols et al., 1973), cat (Abrahams et al., 1987), elephant shrews (Kratzing and Woodall, 1988), and moles (Catania, 2005). Recent studies of vibrissa movements have resulted in several biomechanical models of the vibrissa motor plant that relate muscle activation to the patterns of whisking (Berg and Kleinfeld, 2003; Simony et al., 2010; Haidarliu et al., 2011; Solomon and Hartmann, 2011). Yet the motile aspect of the structure of the *Rhinarium* remains to be characterized.

In rodents, *Rhinarium* movements are involved in the functioning of the two sensory modalities: active tactile sensing (Catania, 2005; Kleinfeld et al., 2006), and active olfactory

[*]Correspondence: Dr. Sebastian Haidarliu, Department of Neurobiology, The Weizmann Institute of Science, Rehovot 76100, Israel, Tel. 972-8-9342192, Fax 972-8-9346099, sebastian.haidarliu@weizmann.ac.il.

sensing (Wachowiak, 2011; Haidarliu et al., 2012). Active tactile sensing is achieved by facilitation of the object touch by narial pads. These pads are densely innervated (Macintosh, 1975; Silverman et al., 1986), and are coated with glabrous skin that is topped by epidermal ridges, known as rhinoglyphics (Hill, 1948). Olfaction is based on air sampling by the nostrils during sniffing (Wilson and Sullivan, 1999; Kepecs et al., 2006). Further, nose-to-nose touch may transmit behaviorally important information that can alter subsequent social interactions in rats (Wolfe et al., 2011). Other mammals that possess *Rhinaria* and associated musculature, appear to use them for more restricted behaviors. Coati use their *Rhinaria* for tactile exploration (Barker and Welker, 1969), moles, for searching for food (Catania, 2005), Suoidea, for manipulations with force application (Herring, 1972). Lastly, in mammals, such as the hairy-nosed otter and wombat, short hairs cover the *Rhinaria* (Triggs, 1996; Nguyen et al., 2001), which suggest that the *Rhinarium* cannot mediate tactile sensing by direct touch.

In the rat, the movable part of the nose is short, amplitudes of the movements are small, and the densely innervated surface of the *Rhinarium* is restricted to two small narial pads. Nevertheless, these narial pads are used for tactile exploration of rostrally-located objects. Rats turn their noses in different directions during exploratory behavior and sniffing and, prior to taking decisions, they touch the objects with their *Rhinarium* (Welker, 1964; Bracha et al. 1990). Structural features that can enable the rat nose, *Rhinarium*, and narial pads to change their shape and touch objects appeared to be interconnected. These include the nasofacial musculature and the cartilaginous nasal capsule (Wang et al., 1994; Maier, 2000) also referred to as the nasal cartilaginous skeleton (NCS) (Mess, 1999; Banke et al., 2002).

Recently, we determined the origins and insertion sites of several nasofacial muscles to evaluate their participation in vibrissa movements and control of the spatial patterns of nasal air conducting pathways (Haidarliu et al., 2010, 2012). The role of these muscles in whisking and general airflow control has been discussed (Deschênes et al., 2012; Moore et al., 2013). Here we seek to understand how rats achieve highly motile movements with their nose as well as movements common to whisking and sniffing. We determine the typical geometry of the nasal musculature and configuration of the cartilaginous structures of the outer nose, as well as their participation in spatial changes of the nose tip position. Further, the relationships between the NCS and the bony skeleton are examined to determine whether and how they contribute to active touch by *Rhinarium* and narial pads.

MATERIALS AND METHODS

The morphology of the *Rhinarium* and the basis of its high mobility were examined by histoenzymatic and histochemical methods that reveal anatomical structures *in situ*, without affecting tissue morphology during processing. All the experimental procedures were conducted according to NIH standards, and were approved by the Institute Animal Care and Use Committee at the Weizmann Institute of Science. Tissue samples were obtained from six one-week-old, four two-week-old, four three-week-old, ten twelve-fourteen-week-old, three nine-month-old and four one-year-old male albino Wistar rats. After slicing the tissue samples with a microtome, striated muscles were visualized in even numbered slices by histoenzymatically revealing cytochrome oxidase activity as recently described (Haidarliu et

al., 2010). Nasal cartilages were identified and their relationships with the other snout structures determined in odd numbered slices histochemically. Nose retraction/protraction and vibrissa position in behaving rats was determined simultaneously using a regular Olympus camera (FE-330). Rhinarial morphology in head-fixed rats was visualized with a binocular digital stereo microscope (Labomed DigiStar, Labo America Inc., Port Myers, Florida, USA).

Histoenzymatic staining for cytochrome oxidase

After euthanasia with Penthal (0.6 mL/kg body weight, i.p.), transcardial perfusion of rats was performed with 4 % (w/v) paraformaldehyde and 5 % (w/v) sucrose in 100 mM phosphate buffer (pH 7.4). After perfusion, the rostral part of the snout was excised and postfixed in the perfusion solution with 30 % (w/v) sucrose. After 48 hours of postfixation, each tissue sample was sectioned into 30 μm thick slices in the coronal, tangential, or horizontal planes using a sliding microtome (SM 2000R, Leica Instruments, Germany) coupled to a freezing unit (K400, Micron International, Germany). Slices in which cytochrome oxidase activity was to be revealed were treated according to our modification (Haidarliu and Ahissar, 2001) of a procedure by Wong-Riley (1979). Briefly, free-floating slices were incubated in an oxygenated solution of 4 % (w/v) sucrose, 0.02 % (w/v) cytochrome *c* (Sigma-Aldrich, St. Louis, MO, USA), catalase (200 μg/mL), and 0.05 % (w/v) diaminobenzidine in 100 mM phosphate buffer for two to three hours at room temperature under constant agitation. Upon clear differentiation between highly-reactive and non-reactive tissue structures, the incubation was arrested by rinsing with 100 mM phosphate buffer. Stained slices were mounted on slides, cover-slipped with Krystalon (Harleco; Lawrence, KS), and examined by light microscopy. Striated muscles appeared as dark-brown bundles in the rostral part of the rat head.

Histochemical staining for cartilage

In mammals, the nasal septum and entire NCS are composed of hyaline cartilage (Naumann et al., 2002; Popko et al., 2007). The hyaline cartilage of the NCS was stained with Alcian blue, which stains extracellular matrix (ECM) blue, reveals different zones of hyaline cartilage (Conklin, 1963), and can bind to proteoglycans proportionally to their concentration (Ippolito et al., 1983). Since tissue components, such as cytoplasm, nuclei, and fibers are not stained by Alcian blue, we counterstained with Thiazine red to visualize these structures. Thiazine red has a high affinity for fibrillary structures (Uchihara et al., 2000), stains myosins and epithelial cells, and emits orange (550 nm) fluorescence (Puchtler et al., 1974; Bacskai et al., 2003).

Odd-numbered, 30 μm-thick slices, which remained unstained after staining for cytochrome oxidase activity, were mounted on slides, dried in air, and then stained for 30 minutes with 0.2 % (w/v) Alcian blue 8GX (Sigma-Aldrich) at room temperature. The slices were washed with distilled water, and counterstained with 1 % (w/v) Thiazine red for one minute at room temperature. After which, the slices were washed with distilled water, dehydrated in sequential solutions of 50, 70, 95 % (w/v) and absolute ethanol, cleared in xylene, and cover-slipped with Krystalon. Some sections were also stained with Methylene blue, Neutral red, or Cresyl violet (Haidarliu and Ahissar, 1997).

Stained slices were examined using a Nikon Eclipse 50i microscope. Bright-field and/or epifluorescence images were imported into Adobe Photoshop software. Only minimal adjustments in the contrast and brightness of the images were made.

We examined whether the combination of Alcian blue with Thiazine red can be useful for differential staining of different types of cartilages, depending on the dominating type of collagen. As a positive control for revealing hyaline and fibrous cartilage, we used slices from the knee of young rats that contain articular hyaline cartilage rich in Type II collagen, and ligaments, such as knee cruciate ligament, and Achilles tendon related to the talocrural joint, which are reported to contain predominantly Type I collagen (Eyre and Wu,1983). The articular hyaline cartilage was extensively stained with Alcian blue. Counterstaining with Thiazine red did not change the blue appearance of the hyaline cartilage, whereas other structures, which contained mostly Type I collagen, appeared red. When the fluorescence of the counterstained slices was examined, the hyaline cartilage did not fluoresce, whereas structures containing Type I collagen as a dominant component, i.e., cruciate ligament, patellar tendon, Achilles tendon, and epidermis, exhibited strong red-yellow fluorescence.

Anatomical description

A uniform description of nasal cartilages and muscles is still lacking (Bruintjes et al., 1996), despite efforts to unify anatomical nomenclature. For the facial muscles, terminology conforming to the *Terminologia anatomica* (1998), with corresponding English equivalents (Whitmore, 1999), was used. Unifying nomenclature for the facial musculature of mammals (Diogo et al., 2009) was also considered. We used cartilage terminology summarized and proposed by Zeller et al. (1993), Ade (1999) and Mess (1999). Most cartilages in the external nasal skeleton, cranial terminology in Chiroptera proposed by Göbbel (2000), and the description of rostral nasal cartilages in soricids (Maier, 2002) appeared relevant for the rat as well. The external rat *Rhinarium* morphology was similar to that of the Lagomorpha described by Ade (1999).

RESULTS

Structural organization of the Rhinarium and NCS

In the rat, the *Rhinarium* is positioned at the rostral-most end of its snout. It involves the nostrils and two symmetric narial pads recently described (Haidarliu et al., 2012). Each narial pad has two asymmetric parts, the *Crus superius* and *the Crus inferius*, similar to those in rabbits (Ade, 1999). The dorsal and ventral borders of the rat's narial pads are defined by two slender horizontal integumental hairless folds, the lateral borders form the medial edge of the nostrils, and the medial borders are determined by the median sulcus. The surface of the *Crus superius* is covered by semicircular epidermal ridges (Fig. 1). The *Crus inferius* is smaller, and only slightly ridged, mainly at the border with the *Crus superius.* These ridges continue up to the lateral edge of the narial pads.

In the resting state, the tip of the rat nose usually protrudes rostrally beyond the line formed by the outer margin of the upper lip. When the vibrissae protract, the tip of the nose retracts (Welker, 1964). We wondered if the nose retraction relative to the entire head was real or

only apparent, particularly since the upper lip and mystacial pads also can be moved rostrally and result in vibrissa movement described as combined vibrissa and mystacial pad translation (Mehta et al., 2007; O'Connor et al., 2010; Solomon and Hartmann, 2011; and Moore et al., 2013). Turning of the head or unilateral vibrissa-object interaction during whisking leads to whisking and snout asymmetry (Ahissar and Knutsen, 2008; Mitchinson et al., 2011; Grant et al., 2012; Deutsch et al., 2012). Therefore, we dissected the rat rostrum such that the connections of the nasal capsule with the skull were preserved. Dissected NCSs from young, *i.e*., 1 to 2 week-old, and old, *i.e.*, 1 year-old, rats looked similar, except for their size (Fig. 2). The preparations had cylindric shape, with a few prominent structures, such as nasal tectum, dorsal nasal cartilage, and two symmetric cupular cartilages, which were giving a characteristic external appearance of the nasal capsule. When weak manual pressure was applied to the tip of the nose in preparations obtained from adult rats, the rostral end of the nose could be moved in the caudal, dorsal, or ventral directions by ~ 1 mm, and laterally by more than 2 mm. When the pressure ceased, the tip of the nose returned back to its initial resting position.

Relationships of the NCS with the Rhinarium and the skull

Examination of the *Rhinarium* and adjacent structures in histochemical preparations

revealed the anatomical features that can account for described nasal mobility. First, the *Rhinarium* and narial pads moved together with the rostral end of the nose. Second, the narial pads were tightly attached to the cartilaginous lateral ventral process (Fig. 3) and could be separated from the cartilage only by cutting the fibrous tissue that connects them. In contrast, the furry skin covering the remainder of the nose was easily separated from the surface of the cartilage.

All nasal cartilages were assembled within the nasal capsule into a unique cartilaginous ensemble, that was seen in both horizontal (Fig. 3), and coronal (Fig. 4) slices. At the level of the pyriform aperture, the NCS formed a telescopic connection with nasal bones and premaxilla (Figs. 2, 3 and 5), which permitted a shift of the NCS relative to the skull along its rostrocaudal axis, and bending of the nose in the dorsoventral and lateral directions. In the rat skull preparation, the rostral ends of the premaxilla tilted laterally, forming an opening reminiscent of a funnel, which may facilitate turning entire NCS in different directions (Fig. 6). Rostrolateral edges of the nasal bones formed an angle with the premaxilla, with the vertex located approximately 2 mm more caudal than the rostral ends of the nasal bones and of the dorsorostral spine of the premaxilla. Such bone connections permit a larger lateral bending of the NCS relative to its bending in the dorsal and ventral directions.

Intrinsic organization of the NCS

The shape of the nose is maintained by the cartilages of the NCS that are connected to each other directly or by means of intervening connective tissue and fibrous aponeurosis. Within the NCS, septum nasi was positioned in the sagittal plane. It was represented by a blade-shaped hyaline cartilage (Figs. 3 and 5) that had an even thickness along the dorsal (Fig. 7a) and ventral (Fig. 7d) borders, but contained thin areas lacking cartilage, *i.e.*, septal fenestrae,

in the rostral half at the level of nostrils and narial pads (Figs. 3, 5a and 7b,c) that facilitated NCS bending and nose retraction.

The NCS was represented rostrally by cupular cartilage and its lateral ventral process, and continued caudally, along the midline, as the septal cartilage. Dorsally, in caudal direction, cupular cartilages continued as roof cartilages to form, according to Maier (2002) the nasal tectum (Figs. 2 and 4). Laterally, the tectum was connected to the cartilages of the nasal sidewall. At this level, ~3 mm caudal from the *Rhinarium* in adult rats, the cartilage that formed the bottom of the nasal cavity (anterior transverse lamina), was fused with the septal cartilage, and connected to the cartilages of the nasal sidewall, which together with the tectum formed a continuous cartilaginous ring (Fig. 5b4). A similar complete cartilaginous ring, formed by nasal cartilages, was previously observed in Echidna aculeata (Gaupp, 1908) and named *Zona annularis*. This ring was also described in guinea pigs (Dierbach, 1985), mouse lemurs (Lozanoff and Diewert, 1989), and in fetal tamarins (Smith et al., 2008) and tenrecs (Schunke and Zeller, 2010). In other mammals, such as the red squirrel (Slabý, 1991), galago (Kanagasuntheram and Kanan, 1964), and adult tamarins (Mueller, 1981), the *Zona annularis* appeared to be interrupted.

Changes in the configuration of the lateral nasal wall occur mainly in the portion of the NCS that occupies a segment between the nostrils and *Zona annularis*. Along this segment, cartilages of the nasal sidewall were not connected to both the tectum in the dorsal part, and to the anterior transverse lamina in the ventral part (Fig. 6b3). When muscles originating from the nasal sidewall contract, the nasal wall can be extended laterally independently from the rest of the NCS. Such an extension is facilitated by the pliability and resilience of the hyaline cartilage.

Dorsal nasal cartilage

In dissected preparations (Fig. 2), the NCS slips caudally under the dorsal nasal cartilage (DNC), which overhangs the pyriform aperture from the dorsal, and forms a rostral continuation for the nasal bones. This nasal cartilage covers the caudal half of the dorsal surface of the NCS in a visor-like fashion (dorsal nasal cartilage in Figs. 2 and 4).

The DNC may serve a second function. Besides limiting dorsal bending of the NCS, the DNC returns the NCS to the resting position after deflection. It may also play a protective role for such a flexible structure as the NCS, preventing its dorsal surface from mechanical impacts. This cartilage has specific tinctorial properties and fluorescence characteristics. The DNC is composed of two symmetric parts that are fused along the midline. In the ventral half of each part, there is a horizontally positioned and compressed in dorsoventral direction structure consisting of hyaline cartilage (Fig. 4a,b,d), which was not stained with Thiazine red and remained blue color. The dorsal compartment of each part was extensively stained with Thiazine red. These dorsal and ventral compartments were surrounded by a perichondrium that was also stainable with Thiazine red (Fig. 4a,b). Thiazine red staining was detected by light microscopy, and by red fluorescence (Fig. 4f). The blue autofluorescence of the septal cartilage and of both the dorsal and ventral compartments of the DNC was similar (Fig. 4e). Such autofluorescence is generally characteristic for different types of collagen, major components of cartilages (Kutsuna et al., 2010).

Musculature of the NCS

Most parts of the *M. nasolabialis profundus, i.e.*, the *Partes maxillares superficialis et profunda, Pars interna profunda*, Superficial, Pseudointrinsic, and Posterior slips of the *Pars interna*, originate from the nasal sidewall (Figs. 3, 5a,b3, and 8), so their unilateral contraction can move the rostral part of the NCS laterally, change the angle between the axes of the NCS and of the head, translate rostrally corresponding mystacial pad, and modify the pattern of the atrium configuration. Bilateral contraction of these muscles can move entire NCS caudally due to telescopic connection of the NCS with the skull, and translate both mystacial pads rostral due to insertion of these muscles into mystacial pads. The tendon of the *M. dilator nasi* inserts into the aponeurosis above the NCS (Fig. 7a), and can move the rostral part of the NCS and *Rhinarium* in the lateral and/or dorsal directions (Haidarliu et al., 2012).

The rostral set of the Superficial slips of the *Pars interna* (Figs. 5b2, and 9a) may have a special role in rhinarial movements. These muscle bundles originate from the nasal sidewall and ventral surface of the atrioturbinate, rostral to the ostium of the nasolacrimal duct. They are directed dorsally, encompassing the *Cupula nasi* from the lateral and dorsal, and are inserted into the collagenous layer of the skin close to midline, above the *Rhinarium* (Fig. 9b). These muscle slips may retract the skin above the *Cupula nasi*, rotate the *Rhinarium* slightly, and simultaneously raise the base of the atrioturbinate, which may change the pattern of the air conducting pathways in the atrium.

Based on anatomical data about the origins and insertion sites of the rostral-most nasofacial muscles, and on spatial relationships between the muscles, NCS, and *Rhinarium*, a "rhinarial motor plant" consisting of these anatomical structures is proposed. The muscles in this motor plant include the *M. levator rhinarii, M. depressor rhinarii, M. depressor septi nasi, M. dilator nasi*, rostral slips of the *M. transversus nasi*, and six parts/slips that belong to the *M. nasolabialis profundus, i.e., Partes maxillares superficialis et profunda, Pars interna profunda*, and Pseudointrinsic, Superficial, and Posterior slips of the *Pars interna*. The position of all these muscles is schematically shown in Figure 10.

DISCUSSION

Involvement of task-aimed nasofacial muscle clusters in Rhinarium movement

We confirmed that only two nasofacial muscles originate in the *Rhinarium (Mm. levator et depressor Rhinarii)*. However, contraction of these two muscles cannot account for all rhinarial movements. These two small muscles can stretch moderately integumental folds in the vertical direction according to their origin and insertion sites, and simultaneously stabilize the position of narial pads during object touch, and probably only move the *Rhinarium* up or down slightly. The amplitude of *Rhinarium* movements depends on their directions. Vertical movements are limited by two anatomical structures: in the ventral direction, by the dorsorostral spine of the premaxilla, and in the dorsal direction, by the DNC that is connected to the nasal bones and covers the caudal half of the NCS. Horizontal (lateral) rhinarial movements, which do not have such limits, have larger amplitudes. These horizontal movements of the *Rhinarium* can be called "translational" because they are

determined entirely by the deflections of the rostral end of the NCS. Furthermore, these movements may be synchronized with the rostral translation of mystacial pads due to contraction of different parts and slips of the *M. nasolabialis profundus*, because these muscles originate from the nasal sidewall (Posterior and Pseudointrinsic slips of the *Pars interna*, *Pars interna profunda*, and *Partes maxillares superficialis et profunda)*, and are inserted into the mystacial pad. The participation of these muscles in both sniffing (fast breathing) and whisking adds a potential anatomical coupling link to the circuitry that drives breathing (Smith et al., 1991) and whisking (Moore et al., 2013).

The organization of the nasofacial musculature into different motor plants according to their spatial arrangement and sensory tasks can be summarized (Table 1) based on data by Hill et al. (2008) about the vibrissa motor plant, and data about arrangement of the muscles in the mystacial pad (Haidarliu et al., 2010) and their participation in active olfactory sensing during sniffing (Haidarliu et al., 2012). The rhinarial motor plant is served by 11 muscles or muscle slips, of which seven are shared with both vibrissal and nasal olfactomotor plants, two are shared only with the olfactomotor plant, and two are only involved in rhinarial movements (*M. levator and M. depressor rhinarii)*. The vibrissal motor plant is served by all intrinsic and 12 extrinsic (for mystacial pad) muscles, while the nasal olfactomotor plant is served by 11 nasofacial muscles. The nasal olfactomotor and vibrissa motor plants share seven muscles.

Since most nasofacial muscles that belong to different motor plants can perform different tasks during their contraction can explain why *Rhinarium*, from which only two muscles originate, can move in different directions in 3D space. This enables the *Rhinarium* to perform an active tactile sensing by touching objects, and to be involved in other coordinated movements, such as sniffing and airflow control.

Recently, few rat models aimed to accelerate recovery after facial nerve injury were developed (Angelov et al., 2007; Guntinas-Lichius et al., 2007; Hadlock et al., 2010; Heaton et al., 2013). In these models, mystacial pad was chosen as a target for mechanical stimulation. We suggest that NCS also may serve as a similar target. We found that rhinarial motor plant possesses muscles that originate from the NCS and insert into mystacial pads. Presumably, movements of the NCS force to move mystacial pads as well. To move NCS, mechanical stimulation or inhalation of chemical agents that provoke sniffing can be used. Sniffing is accompanied by simultaneous oppositely phased repetitive retraction and protraction of the tip of the nose and of the mystacial vibrissae (Welker, 1964). Due to reciprocating rostrocaudal movements of the NCS during sniffing, mystacial pads can move synchronously. Consistent controlled sniffing/whisking can be evoked, for example, by inhalation of peanut butter or isopropyl alcohol (Heaton et al., 2008).

Nasal cartilages as mediators of rhinarial movements

In rodents, the nose participates in active tactile and olfactory sensing, functions reflected in the nose anatomy. Nasal and rhinarial mobility, which is functionally important, is controlled by the movement of the rostral end of the NCS. The NCS was initially described in bats (Grosser, 1902), and later in many other mammals, including shrews (Katzing and Woodall, 1988), rabbits (Mess, 1999), and mole rats (Banke et al., 2002). In rabbits,

cartilages of the NCS are hyaline cartilages, which have the highest stiffness and unique pattern of collagen composition (Naumann et al., 2002). We suggest that the NCS determines nasal shape, rhinarial movements, narial pad active touch, and the pattern of air conducting pathways within the *Vestibulum nasi* in the same manner as colllagenous skeleton of the rat mystacial pad determines the anatomical and functional integrity of the entire mystacial pad.

The morphology of the DNC in rats is described here for the first time. Whereas most cartilages in the body are gradually replaced by bone, the rostral part of the nasal septum, which is centrally located in the NCS, remains cartilaginous throughout the life of mammals (Scott, 1953). Similarly, here we observed that in aged rats cartilages in the entire NCS and the DNC overlying it retained their flexibility and had a similar appearance and proportions as in young rats (Fig. 2), without signs of ossification. The structural organization of the DNC reflects its functional properties. The caudal end of this cartilage is connected to the nasal bones. Although this cartilage has no direct connections with the muscles, it is constantly subjected to mechanical action by the dorsal surface of the NCS when the latter is moving or bending. The dorsal movement of the NCS may be damped and limited by the DNC. These two structures are linked together by connective tissue that forms a nasal aponeurosis. When the muscles that moved the NCS in whatever direction become relaxed, DNC facilitates the return of the NCS to the resting position. This occurs because the core of the DNC contains resilient hyaline cartilage that works like a spring and damper, and is surrounded by a layer of fibrous cartilage with stretching and shock-absorbing properties. We suggest that other mammals also may possess similar complementary cartilaginous structures which can protect NCS from mechanical impacts and/or regulate using their *Rhinarium* for active tactile sensing by the nose.

The different tinctorial properties of the cartilage of the DNC compared to that of the NCS (Fig. 4) may account for the DNC not being observed in previous studies. When slices were stained with Alcian blue and then counterstained with other dyes, such as Neutral red, Methylene blue, Cresyl violet or Thiazine red, only Thiazine red did not stain the NCS. With Thiazine red, the blue color of the alcianophilic hyaline cartilage remained unchanged, while other structures that contained mainly Type I collagen were extensively stained (Figs. 3 and 4). Cresyl violet and Neutral red, like Alcian blue, have a high affinity for hyaline cartilage. They extensively stain only hyaline cartilage in the NCS and DNC, and not the dorsal area of the DNC (Fig. 11). Cationic dyes, such as Alcian blue and Neutral red, were reported to bind to structures that contain glycosaminglycans (Sulzer and Holtzman, 1986).

Alcian blue selectively stained the extracellular matrix of all the cartilages of the NCS, and only the ventral part of the core of the DNC (Fig. 4a,b). This tinctorial dissimilarity of the NCS and DNC can be explained by the presence of different collagen types. Type I collagen is present in fibrous (tendinous) tissues and fibrocartilage, whereas Type II collagen is characteristic of the extracellular matrix of the hyaline cartilage (Mizoguchi et al., 1992; Filova et al., 2010), and accounts for about two-thirds of the dry weight of articular hyaline cartilage (Buckwalter and Mankin, 1998; Eyre, 2002). Blue autofluorescence, caused by all the types of collagen, was similar for the NCS and for both parts of the DNC (Fig. 4e), whereas red fluorescence after staining with Thiazine red occurred only in the dorsal part

and in the fibrous perichondrial envelope of the DNC, and was absent in the NCS and in the ventral part of the DNC (Fig. 4f). These findings agree with those of Mizoguchi et al. (1992) who found that Type II collagen is characteristic for the septal cartilage, while Type I collagen is absent in the extracellular matrix of septal cartilage.

Narial pads play a central role in active tactile sensing by the nose. The pads are attached to the rostral end of the NCS that is represented by an ensemble of cartilages that exhibit certain mobility when a behaving animal moves its nose and/or interacts with objects. Such mobility and flexibility of the rostral part of the rat snout is provided by a telescopic connection between the NCS and the nasal and premaxilla bones that form the entrance (pyriform aperture) for the NCS into the nasal cavity of the skull, and by the ability of the NCS to bend along its rostrocaudal axis. Nasofacial muscles of the rat snout can move the entire NCS, together with the *Rhinarium*, in the caudal direction. However, in the rat, the role of the telescopic anatomical connection between the NCS and the bony walls of the pyriform aperture is minimal for *Rhinarium* retraction, being limited to ~1 mm because of the strong fasciae that connect the dorsal and ventral parts of the NCS to the bones. Dorsoventral deflections of the rostral end of the NCS are also of small amplitudes because dorsally, the DNC extends rostrally from the nasal bones (Fig. 2), and ventrally, the prominent dorsorostral spine of the premaxilla forms the most rostral point of the skull (Fig. 6) and limits ventral deflection of the NCS. In shrews, retraction of the nose is due to telescopic arrangement of the three caudal-most elements of the NCS (Maier, 2002). In other animals, such as Suidae, in which the *Rhinarium* moves and can apply force to objects, movements are due to specific anatomy and special musculature (Herring, 1972).

Telescopic principle of connecting cartilage to the bone that permits to move NCS relative to the skull along its sagittal axis, as well as the ability to produce angular deflections of the nasal capsule may be appropriate for the other animals. Further study of such connections may be useful for understanding mechanisms of nasal motility during active tactile sensing with the nose, as well as for nasal surgery which can use this principle in nose reconstruction after nasal injuries.

Summary

The rostral nasofacial muscles of the rat are functionally organized into task-intended clusters that assist in whisking, sniffing, and rhinarial movements. These can be classified as vibrissa motor, nasal olfactomotor, and rhinarial motor plants, respectively (Table 1). These motor plants are overlapping: each of them involves muscles that are shared with the other motor plants, as well as muscles that perform only one specific task. The *Rhinarium* is tightly attached to the rostral end of the NCS, the motility of which determines rhinarial movements. Movement of the NCS is controlled by rhinarial motor plant, the muscles of which are partially shared by both the vibrissa motor, and nasal olfactomotor plants. Muscles that change the atrioturbinate position and shape, and muscles that dilate nasal air-ways, represent the nasal olfactomotor plant that regulates sniffing parameters by shaping nasal air-conducting pathways.

Acknowledgments

The authors thank Barbara Schick for reviewing the manuscript. Ehud Ahissar holds the Helen Diller Family Professorial Chair of Neurobiology.

Grant support: The Minerva Foundation funded by the Federal German Ministry for Education and Research; The United States National Institutes of Health, Grant number NS058668; The United States – Israel Binational Science Foundation, Grant number 2007121.

Abbreviations

DNC	dorsal nasal cartilage
ECM	extracellular matrix
NCS	nasal cartilaginous skeleton

Literature Cited

Abrahams VC, Hodgins M, Downey D. Morphology, distribution, and density of sensory receptors in the glabrous skin of the rat rhinarium. J Morphol. 1987; 191:109–114. [PubMed: 3560233]

Ade M. External morphology and evolution of the rhinarium in Lagomorpha. With special reference to the Glires hypothesis. Mitt Mus Nat kd Berl, Zool Reihe. 1999; 2:191–216.

Ahissar E, Knutsen PM. Object localization with whiskers. Biol Cybern. 2008; 98:449–458. [PubMed: 18491159]

Angelov DN, Ceynowa M, Guntinas-Lichius O, Streppel M, Grosheva M, Kiryakova SI, Maegele E, Irintchev AP, Neiss WF, Sinis N, Alvanou A, Dunlop SA. Mechanical stimulation of paralyzed vibrissal muscles following facial nerve injury in adult rat promotes full recovery of whisking. Neurobiol Dis. 2007; 26:229–242. [PubMed: 17296303]

Bacskai BJ, Hickey GA, Skoch J, Kajdasz ST, Wang Y, Huang G, Mathis CA, Klunk WE, Hyman BT. Four-dimensional multiphoton imaging of brain entry, amyloid binding, and clearance of an amyloid--β ligand in transgenic mice. PNAS. 2003; 100:12462–12467. [PubMed: 14517353]

Banke, J.; Mess, A.; Zeller, U. Functional morphology of the rostral head region of *Cryptomys hottentotus* (Bathyergidae, Rodentia). In: Denys, C.; Granjon, L.; Poulet, A., editors. African Small Mammals. Paris: IRD Editions; 2002. p. 231-241.

Barker DJ, Welker WI. Receptive fields of first-order somatic sensory neurons innervating rhinarium in coati and raccoon. Brain Res. 1969; 14:367–386. [PubMed: 5794913]

Berg RW, Kleinfeld D. Rhythmic whisking by rat: retraction as well as protraction of the vibrissae is under active muscular control. J Neurophysiol. 2003; 89:104–117. [PubMed: 12522163]

Bracha V, Zhuravin IA, Bures J. The reaching reaction in the rat: a part of the digging pattern? Behav Brain Res. 1990; 36:53–64. [PubMed: 2302321]

Brecht M, Preilowski B, Merzenich MM. Functional architecture of the mystacial vibrissae. Behav Brain Res. 1997; 84:81–97. [PubMed: 9079775]

Bruintjes TD, van Olphen AF, Hillen B. Review of the functional anatomy of the cartilages and muscles of the nose. Rhinology. 1996; 34:66–74. [PubMed: 8876065]

Buckwalter JA, Mankin HJ. Articular cartilage: Tissue design and chondrocyte-matrix interactions. Instr Course Lect. 1998; 47:477–486. [PubMed: 9571449]

Catania KC. Evolution of sensory specializations in insectivores. Anat Rec. 2005; 287A:1038–1050.

Conklin JL. Staining properties of hyaline cartilage. Am J Anat. 1963; 112:259–267. [PubMed: 14022583]

Deschênes M, Moore JD, Kleinfeld D. Sniffing and whisking in rodents. Curr Opin Neurobiol. 2012; 22:243–250. [PubMed: 22177596]

Deutsch D, Pietr M, Knutsen PM, Ahissar E, Schneidman E. Fast feedback in active sensing: touch-induced changes to whisker-object interaction. PLoS One. 2012; 7:e44272. [PubMed: 23028512]

Dierbach AR. Morphogenesis of the cranium of Cavia porcellus L. II. Comparative part and literature. Gegenbaurs Morphol Jahrb. 1985; 131:617–642. [PubMed: 4065513]

Diogo R, Wood BA, Aziz MA, Burrows A. On the origin, homologies and evolution of primate facial muscles, with a particular focus on hominoids and a suggested unifying nomenclature for the facial muscles of the Mammalia. J Anat. 2009; 215:300–319. [PubMed: 19531159]

Eyre D. Collagen of articular cartilage. Arthritis Res. 2002; 4:30–35. [PubMed: 11879535]

Eyre DR, Wu JJ. Collagen of fibrocartilage: A distinctive molecular phenotype in bovine meniscus. FEBS Lett. 1983; 158:265–270. [PubMed: 6688225]

Filova E, Burdikova Z, Rampichova M, Bianchini P, Capek M, Kost'akova E, Amler E. Analysis and three-dimensional visualization of collagen in artificial scaffolds using nonlinear microscopy techniques. J Biomed Optics. 2010; 15:1–7.

Gaupp E. Zur Entwicklungsgeschichte und vergleichenden Morphologie des Schädels von Echidna aculeata var. typica. Semon's Zool Forsch Australien. Denkschr Medicinischnaturwiss Ges Jena. 1908; 6:539–788.

Göbbel L. The external nasal cartilages in Chiroptera: significance for intraordinal relationships. J Mamm Evol. 2000; 7:167–201.

Grant RA, Mitchinson B, Prescott TJ. The development of whisker control in rats in relation to locomotion. Dev Psychobiol. 2012; 54:151–168. [PubMed: 22231841]

Grosser O. Zur Anatomie der Nasenhöhle und des Rachens der einheimischen Chiropteren. Morphol Jahrb. 1902; 29:1–77.

Guntinas-Lichius O, Hundeshagen G, Paling T, Streppel M, Grosheva M, Irintchev A, Skouras A, Alvanou A, Angelova SK, Kuerten S, Sinis N, Dunlop SA, Angelov DN. Manual stimulation of facial muscles improves functional recovery after hypoglossal-facial anastomosis and interpositional nerve grafting of the facial nerve in adult rats. Neurobiol Dis. 2007; 28:101–112. [PubMed: 17698365]

Hadlock T, Lindsay R, Edwards C, Smitson C, Weinberg J, Knox C, Heaton JT. The effect of electrical and mechanical stimulation on the regenerating rodent facial nerve. Laryngoscope. 2010; 120:1094–1102. [PubMed: 20513023]

Haidarliu S, Ahissar E. Spatial organization of facial vibrissae and cortical barrels in the guinea pig and golden hamster. J Comp Neurol. 1997; 385:515–527. [PubMed: 9302104]

Haidarliu S, Ahissar E. Size gradients of barreloids in the rat thalamus. J Comp Neurol. 2001; 429:372–387. [PubMed: 11116226]

Haidarliu S, Simony E, Golomb D, Ahissar E. Muscle architecture in the mystacial pad of the rat. Anat Rec. 2010; 293:1192–1206.

Haidarliu S, Simony E, Golomb D, Ahissar E. Collagenous skeleton of the rat mystacial pad. Anat. Rec. 2011; 294:764–773.

Haidarliu S, Golomb D, Kleinfeld D, Ahissar E. Dorsorostral snout muscles in the rat subserve coordinated movement for whisking and sniffing. Anat Rec. 2012; 295:1181–1191.

Heaton JT, Knox C, Malo J, Kobler JB, Hadlock TA. A system for delivering mechanical stimulation and robot assisted therapy to the rat whisker pad during facial nerve regeneration. IEEE Trans Neural Syst Rehabil Eng. 2013 (Epub ahead of print).

Herring SW. The facial musculature of the Suoidea. J Morph. 1972; 137:49–62. [PubMed: 5032558]

Hill WCO. An undescribed structure in the rodent rhinarium. Nature. 1948; 161:276–277.

Hill DN, Bermejo R, Zeigler HP, Kleinfeld D. Biomechanics of the vibrissa motor plant in rat: rhythmic whisking consists of triphasic neuromuscular activity. J Neurosci. 2008; 28:3438–3455. [PubMed: 18367610]

Ippolito E, Pedrini VA, Pedrini-Mille A. Histochemical properties of cartilage proteoglycans. J Histochem Cytochem. 1983; 31:653–661.

Kanagasuntheram R, Kanan CV. The chondrocranium of a 19 mm C.R. length embrio of Galago senegalensis senegalensis. Acta Zool. 1964; 45:107–121.

Kepecs A, Uchida N, Mainen ZF. The sniff as a unit of olfactory processing. Chem Senses. 2006; 31:167–179. [PubMed: 16339265]

Kleinfeld D, Ahissar E, Diamond ME. Active Sensation: Insights from the rodent vibrissa sensorimotor system. Curr Opin Neurobiol. 2006; 16:435–444. [PubMed: 16837190]

Kratzing JE, Woodall PF. The rostral nasal anatomy of two elephant shrews. J Anat. 1988; 157:135–143. [PubMed: 3198474]

Kutsuna T, Sato M, Ishihara M, Furukawa KS, Nagai T, Kikuchi M, Ushida T, Mochida J. Noninvasive evaluation of tissue-engineered cartilage with time-resolved laser-induced fluorescence spectroscopy. Tissue Eng. 2010; 16:365–373.

Lozanoff S, Diewert VM. Developmental morphology of the solum nasi in the mouse lemur (Microcebus murinus). J Morphol. 1989; 202:409–424. [PubMed: 2600973]

Macintosh SR. Observations on the structure and innervations of the rat snout. J Anat. 1975; 119:537–546. [PubMed: 1141053]

Maier, W. Ontogeny of the nasal capsule in cercopitecoids: a contribution to the comparative and evolutionary morphology of catarrhines. In: Whitehead, PF.; Jolly, CJ., editors. Old World Monkeys. Cambridge: Cambridge University Press; 2000. p. 99-132.

Maier W. Zur funktionellen Morphologie der rostralen Nasenknorpel bei Soriciden. Mamm Boil. 2002; 67:1–17.

Mehta SB, Whitmer D, Figueroa R, Williams BA, Kleinfeld D. Active spatial perception in the vibrissa scanning sensorimotor system. PLoS Biol. 2007; 5:e15. [PubMed: 17227143]

Mess A. The evolutionary differentiation of the rostral nasal skeleton within Glires. A review with new data on Lagomorph ontogeny. Mitt Mus Nat kd Berl, Zool Reihe. 1999; 75:217–228.

Mitchinson B, Grant RA, Arkley K, Rankov V, Perkon I, Prescott TJ. Active vibrissal sensing in rodents and marsupials. Phil Trans R Soc B. 2011; 366:3037–3048. [PubMed: 21969685]

Mizoguchi I, Nakamura M, Takahashi I, Kagayama M, Mitani H. A comparison of the immunohistochemical localization of type I and type II collagens in craniofacial cartilages of the rat. Acta Anat. 1992; 144:59–64. [PubMed: 1514361]

Moore JD, Deschênes M, Furuta T, Hubert D, Smear MC, Demers M, Kleinfeld D. Hierarchy of orofacial rhythms revealed through whisking and breathing. Nature. 2013; 469:53–58.

Mueller D. Beitrag zur craniogenese vom Sanguineeus tamarin Link, 1795 (Platyrrhini, primates). Cour Forach Inst Senkenberg. 1981; 46:1–100.

Naumann A, Dennis JE, Awadallah A, Carrino DA, Mansour JM, Kastenbauer E, Caplan AI. Immunochemical and mechanical characterization of cartilage subtypes in rabbit. J Histochem Cytochem. 2002; 50:1049–1058. [PubMed: 12133908]

Nguyen XD, Pham TA, Le HT. New Information about the Hairy-Nosed Otter (Lutra sumatrana) in Vietnam. IUCN Otter Spec. Group Bull. 2001; 18(2):64–75.

O'Connor DH, Clack NG, Huber D, Komiyama T, Myers EW, Svoboda K. Vibrissa-based object localization in head-fixed mice. J Neurosci. 2010; 30:1947–1967. [PubMed: 20130203]

Popko M, Bleys RLAW, DeGront J-W, Huizing EH. Histological structure of the nasal cartilages and their perichondrial envelopeI. I. The septal and lobular cartilage. Rhinology. 2007; 45:148–152. [PubMed: 17708463]

Pubols BH, Donovick PJ, Pubols LM. Opossum trigeminal afferents associated with vibrissa and rhinarial mechanoreceptors. Brain Behav Evol. 1973; 7:360–381. [PubMed: 4721660]

Puchtler H, Waldrop FS, Carter MG, Valentine LS. Investigation of staining, polarization and fluorescence microscopic properties of myoepithelial cells. Histochem. 1974; 40:281–289.

Schunke AC, Zeller U. Chondrocranium and dermal bones of the lowland streaked tenrec *Hemicentetes semispinosus* (Afrosoricida, Tenrecidae) and their comparison with *Potamogale* and other insectivoran-grade placental mammals. Vertebrate Zool. 2010; 60:37–72.

Scott JH. The cartilage of the nasal septum. Br Dent J. 1953; 95:37–43.

Silverman RT, Munger BL, Halata Z. The sensory innervations of the rat rhinarium. Anat Rec. 1986; 214:210–225. [PubMed: 3954078]

Simony E, Bagdasarian K, Herfst L, Brecht M, Ahissar E, Golomb D. Temporal and spatial characteristics of vibrissa responses to motor commands. J Neurosci. 2010; 30:8935–8952. [PubMed: 20592215]

Slabý O. The nasal apparatus of the red squirrel (Sciurus vulgaris L.) embryo at the stage of the fully formed chondrocranium. Funct Dev Morphol. 1991; 1:61–80. [PubMed: 1790345]

Smith JC, Ellenberger HH, Ballanyi K, Richter DW, Feldman JL. Pre-Bötzinger complex: a brainstem region that may generate respiratory rhythm in mammals. Science. 1991; 254:726–729. [PubMed: 1683005]

Smith SC, Monie IW. Normal and abnormal nasolabial morphogenesis in the rat. Teratology. 1969; 2:1–12. [PubMed: 5788824]

Smith TD, Rossie JB, Docherty BA, Cooper GM, Bonar CJ, Silverio AL, Burrows AM. Fate of the nasal capsular cartilages in prenatal and perinatal tamarins (Saguinus geoffroyi) and extent of secondary pneumatization of maxillary and frontal sinuses. Anat Rec. 2008; 291:1397–1413.

Solomon JH, Hartmann MJZ. Radial distance determination in the rat vibrissal system and the effects of Weber's law. Phil Trans R Soc B. 2011; 366:3049–3057. [PubMed: 21969686]

Sulzer D, Holtzman E. Alcian blue and Neutral red staining of retinal synaptic layers. J Histochem Cytochem. 1986; 34:1513–1515. [PubMed: 2430011]

Thieme, G., editor. Terminologia Anatomica. Federative committee on anatomical terminology. Stuttgard: 1998.

Triggs, B. The wombat: common wombats in Australia. Sydney (Australia): UNSW Press; 1996. p. 141

Uchihara T, Nakamura A, Yamazaki M, Mori D. Tau-positive neurons in corticobasal degeneration and Alzheimer's disease – distinction by thiazin red and silver impregnation. Acta Neuropathol. 2000; 100:385–389. [PubMed: 10985696]

Wachowiak M. All in a sniff: olfaction as a model of active sensing. Neuron. 2011; 71:962–973. [PubMed: 21943596]

Wang R-G, Jiang S-C, Gu R. The cartilaginous nasal capsule and embryonic development of human paranasal sinuses. J Otolaryngol. 1994; 23:239–243. [PubMed: 7996621]

Welker WI. Analysis of sniffing of the albino rat. Behavior (Leiden). 1964; 22:223–244.

Whitmore I. Terminologia Anatomica: new terminology for the new anatomist. Anat Rec (New Anat). 1999; 257:50–53.

Wilson DA, Sullivan RM. Respiratory airflow pattern at the rat's snout and an hypothesis regarding its role in olfaction. Physiol Behav. 1999; 66:41–44. [PubMed: 10222471]

Wolfe J, Mende C, Brecht M. Social facial touch in rats. Behav Neurosci. 2011; 125:900–910. [PubMed: 22122151]

Wong-Riley M. Changes in the visual system of monocularly sutured or enucleated cats demonstrable with cytochrome oxidase histochemisstry. Brain Res. 1979; 171:11–28. [PubMed: 223730]

Zeller U, Wible JR, Elsner M. New ontogenetic evidence of the septomaxilla of Tamandua and Choloepus (Mammalia, Xenarthra), with a reevaluation of the homology of the mammalian septomaxilla. J Mammal Evol. 1993; 1:31–46.

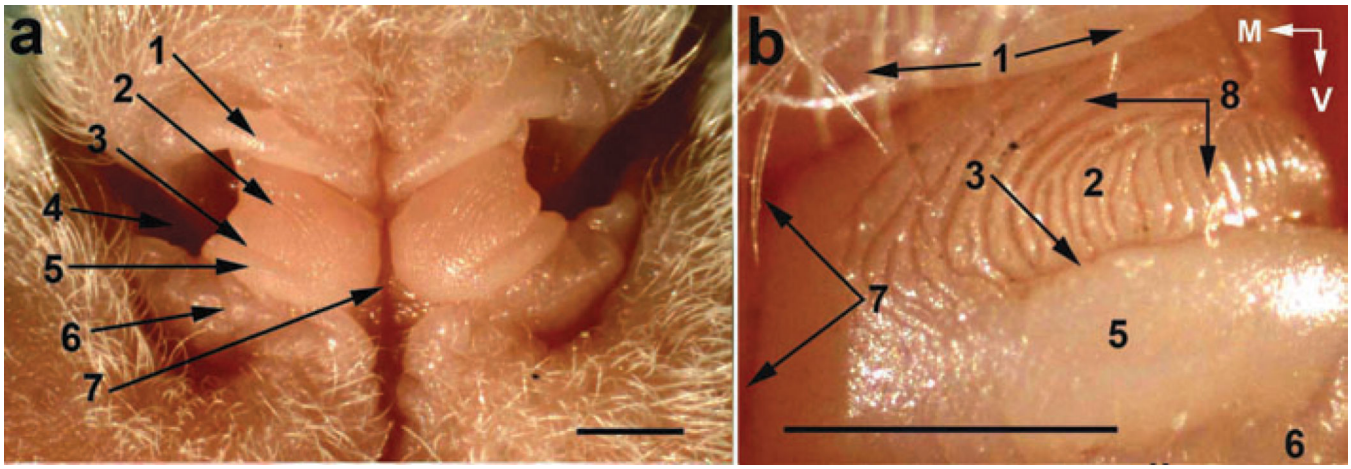

Figure 1.

Light microscopy of the entire *Rhinarium* (a) and left narial pad (b) of an adult rat. (1) Dorsal integumental fold; (2) *Crus superius* of the narial pad; (3) horizontal groove; (4) external nasal opening; (5) *Crus inferius* of the narial pad; (6) ventral integumental fold; (7) median sulcus; (8) epidermal ridges. M, medial; V, ventral. Scale bars = 1 mm.

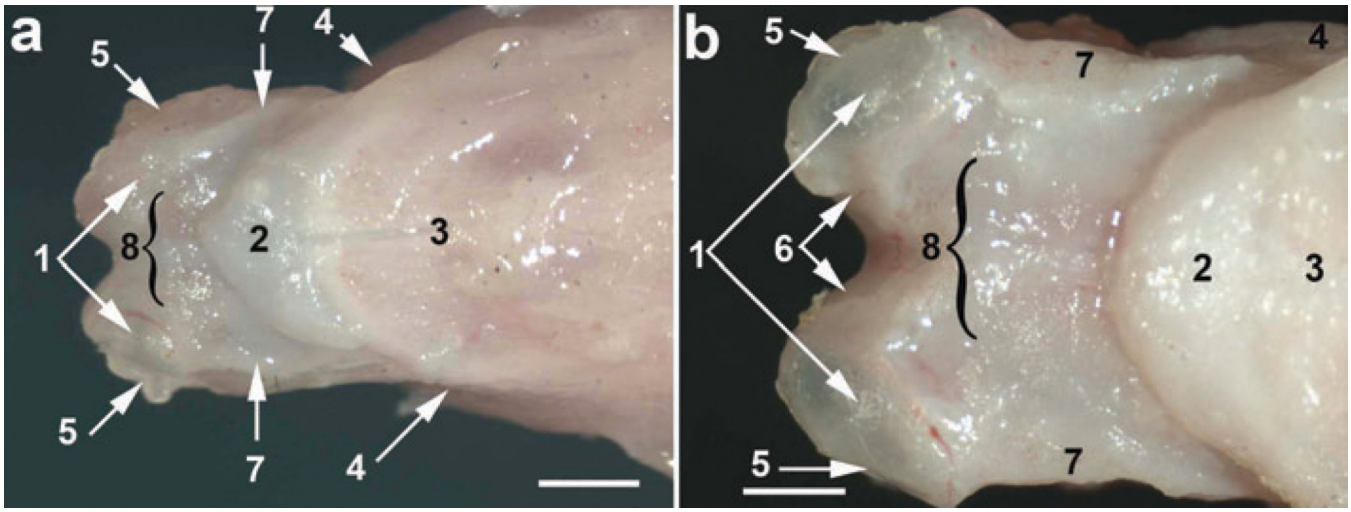

Figure 2.

Dorsal views of the nasal cartilaginous skeleton in a 2-week-old (a) and a 1-year-old (b) rats. (1) Cupular cartilage; (2) dorsal nasal cartilage attached to the nasal bones (3); (4) premaxilla; (5) external nasal opening; (6) lateral ventral process; (7) nasal sidewall; (8) nasal tectum. Scale bars = 1 mm.

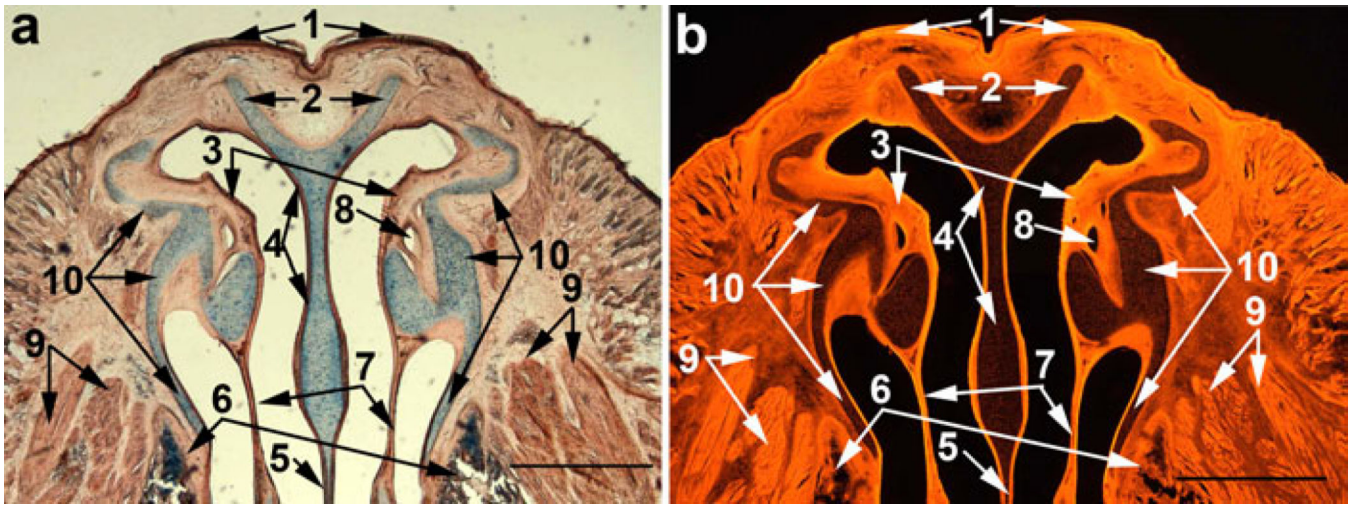

Figure 3.

Light microscopy (a) and fluorescence (b) of a horizontal slice of the nasal cartilaginous skeleton of a one-week-old rat after staining with Alcian blue and counterstaining with Thiazine red. (1) Narial pads; (2) lateral ventral process; (3) atrioturbinate; (4) septum; (5) septal fenestra; (6) premaxilla; (7) maxilloturbinate; (8) ostium of the nasolacrimal canal; (9) nasofacial muscles attached to the nasal sidewall; (10) nasal cartilaginous skeleton. Scale bars = 1 mm.

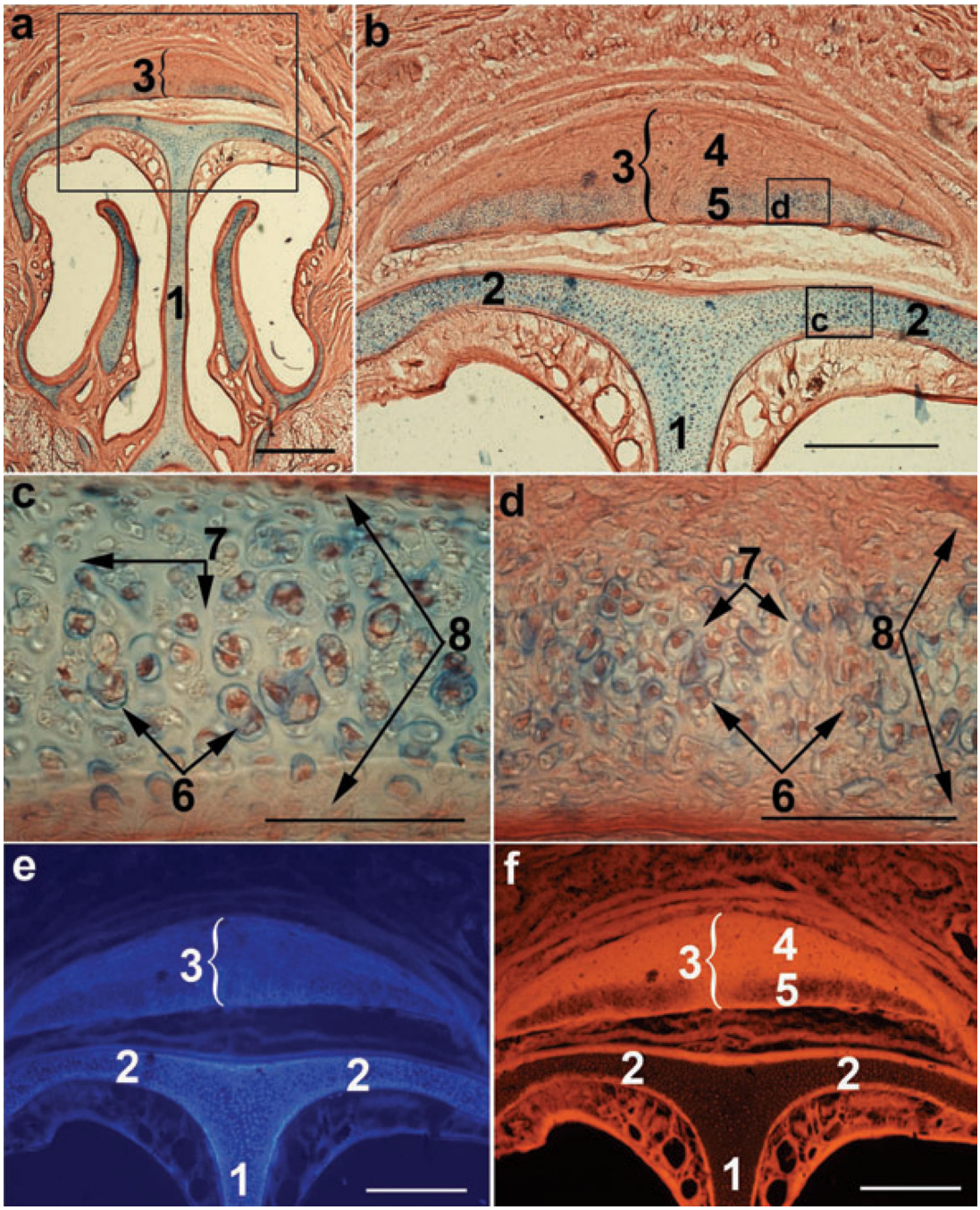

Figure 4.

Light microscopy and fluorescence of nasal cartilages of an adult rat. (a) Coronal slice of the entire nasal cartilaginous skeleton stained with Alcian blue and counterstained with Thiazine red. (b) Boxed area in (a). Boxed areas in (b) represent roof cartilage (c) and the ventral area/compartment of the dorsal nasal cartilage (d). (e), (f) Blue autofluorescence and Thiazine red fluorescence, respectively, of the area shown in (b). (1) Septum; (2) roof cartilage; (3) dorsal nasal cartilage; (4) dorsal and (5) ventral compartments of the dorsal

nasal cartilage; (6) chondrocytes clustered in groups; (7) matrix; (8) perichondrium. Scale bars are 1 mm (a), 0.5 mm (b, e and f), and 0.1 mm (c, d).

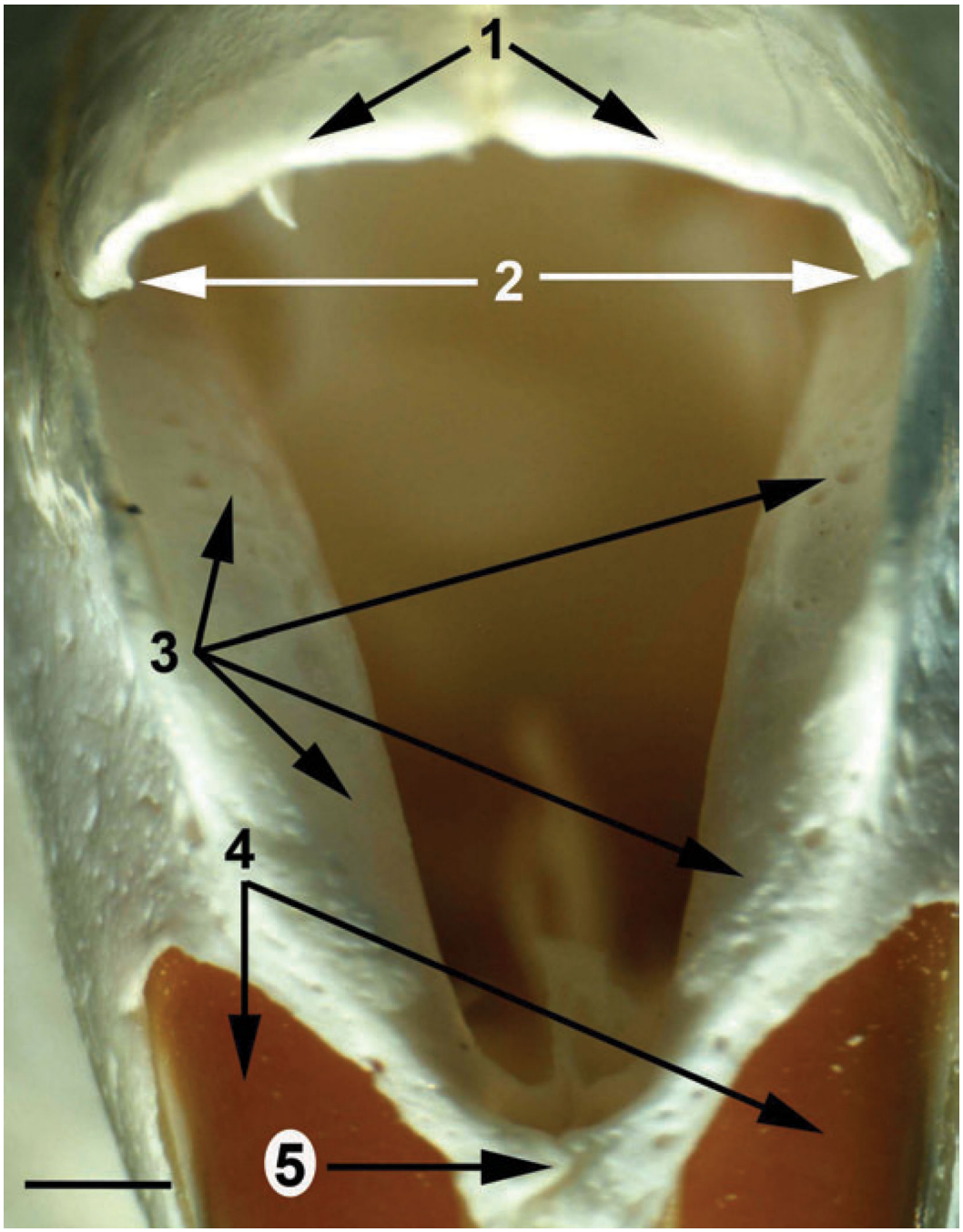

Figure 5.

Light microscopy of horizontal and coronal slices of the rat snout stained for cytochrome oxidase activity. (a) A horizontal slice cut through the snout of a 17-day-old rat at the ventral margin of the nostril. (b) Light microscopy of the coronal slices cut at the positions shown at the bottom of the panel (a). (1) atrioturbinate; (2) rostral edge of the atrioturbinate; (3) narial pads; (4) ostium of the nasolacrimal duct; (5) lateral ventral process; (6) septal *Fenestrae*; (9) fragments of the intraturbinate muscles; (10) the bone of the maxilloturbinate; (11)

rostral edge of the premaxilla; (12) caudal part of the nasal cartilaginous skeleton. Scale bars = 1 mm.

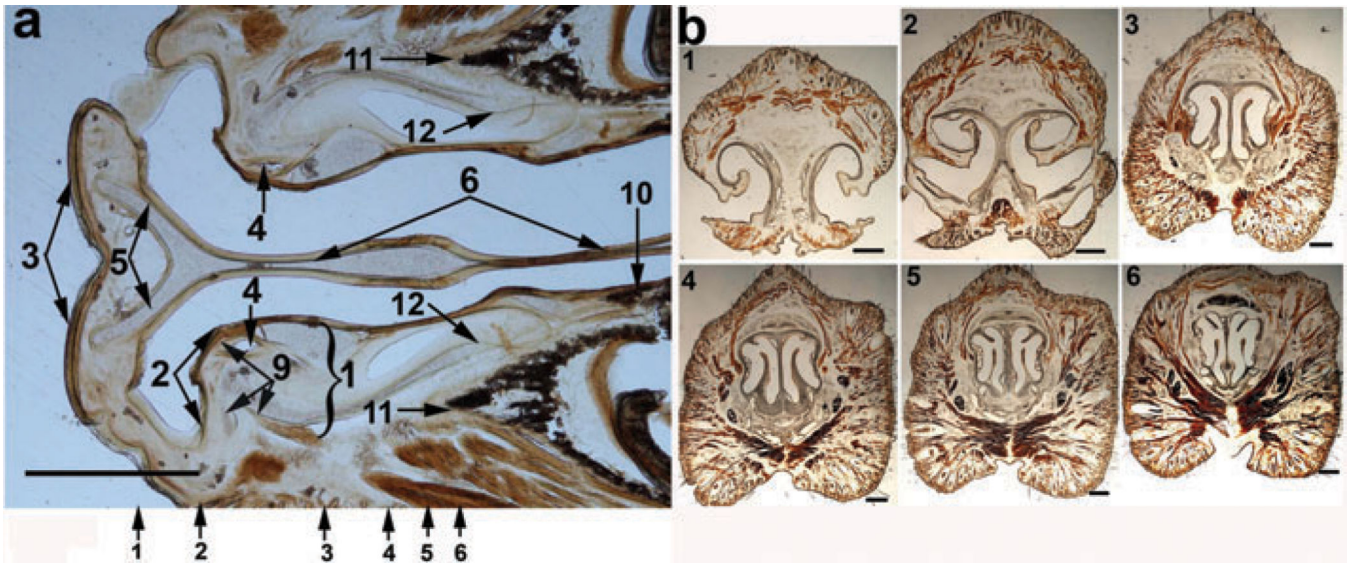

Figure 6.

Light microscopy of the rostral walls of the pyriform aperture in an adult rat skull preparation. (1) Nasal bones; (2) vertex of the angle formed by rostral edges of the nasal bones and premaxilla; (3) the slope (funnel) formed by the rostrolateral edge of the premaxilla; (4) incisives; (5) dorsorostral spine of the premaxilla. Scale bar = 1 mm.

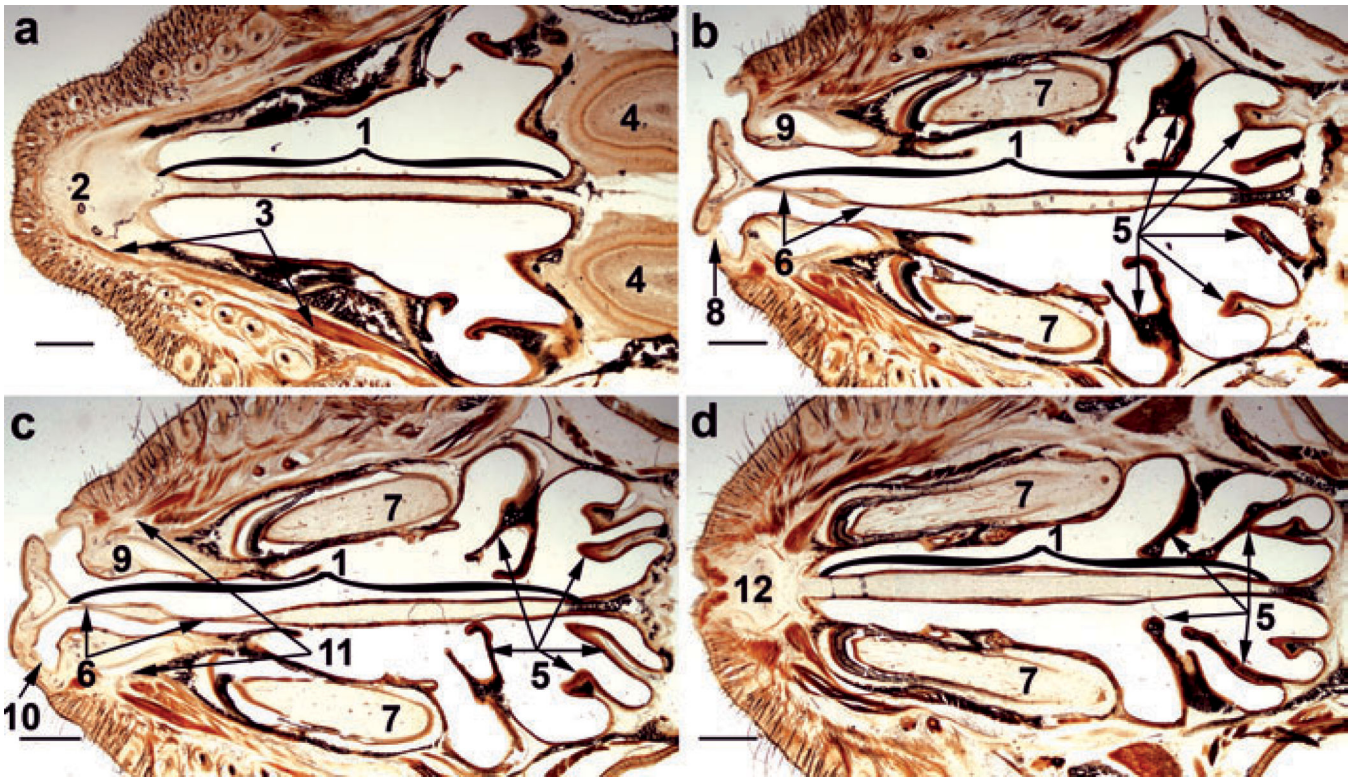

Figure 7.

Light microscopy of stained for cytochrome oxidase activity horizontal slices of the rostral part of the one-week-old rat snout in the dorsal part of the nasal cavity (a), at the level of nostrils and narial pads [(b) and (c), respectively], and at the level of anterior transverse lamina (d). (1) Septum; (2) aponeurosis above *Cupula nasi; (3) M. dilator nasi; (4)* olfactory bulb *; (5)* ethmoturbinates; *(6) Fenestrae septi nasi*; (7) incisives; (8) dorsal edge of the nostril; (9) atrioturbinate; (10) ventral edge of the nostril; (11) sites of muscle attachments to the nasal sidewall; (12) anterior transverse lamina. Scale bars = 1 mm.

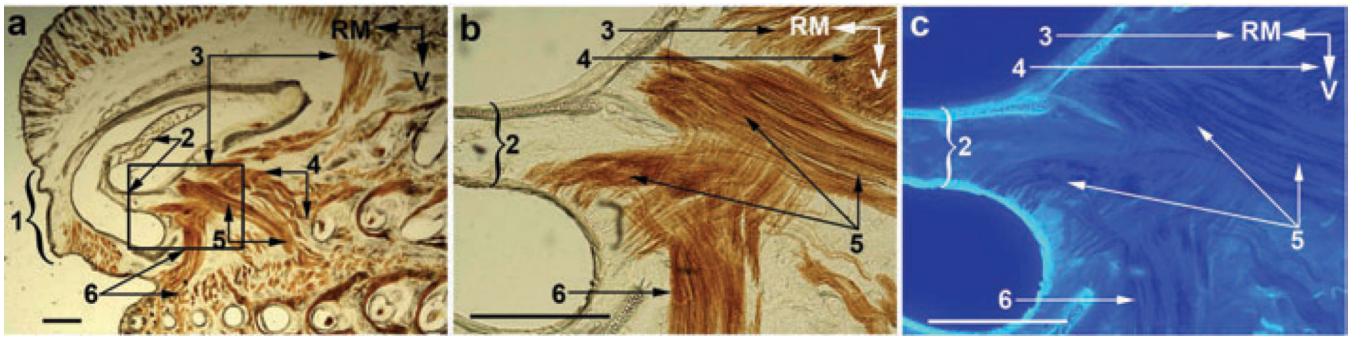

Figure 8.

Muscle attachments to the cartilages of the nasal sidewall. (a, b) Light microscopy and (c) blue autofluorescence; (b) and (c) represent boxed area in (a). (1) *Rhinarium*; (2) atrioturbinate; (3), (4) and (5) Superficial, Pseudointrinsic and Posterior slips of the *Pars interna*, respectively, and (6) *Pars anterior* of the *M. nasolabialis profundus*. RM, rostromedial; V, ventral. Scale bars = 1 mm.

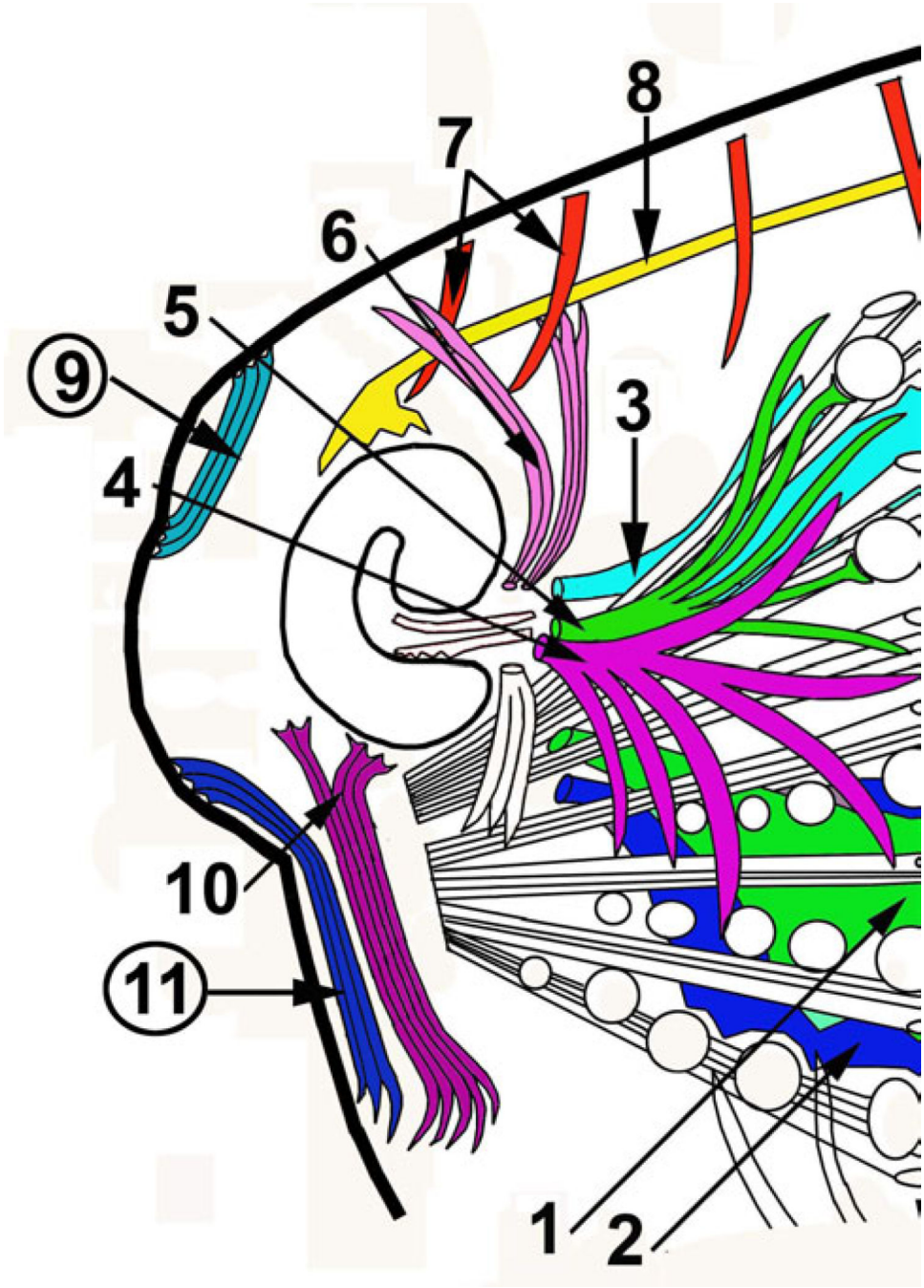

Figure 9.

Light microscopy of a coronal (a) and a tangential (b) slices of the rostral part of the rat snout stained for cytochrome oxidase activity. (1) Superficial slips of the *Pars interna* of the *M. nasolabialis profundus*; (2) *Cupula nasi*; (3) atrioturbinate; (4) *Rhinarium*; (5) nasal sidewall. A4 and B4, vibrissal follicles; RM, rostromedial; V, ventral. Scale bars = 1 mm.

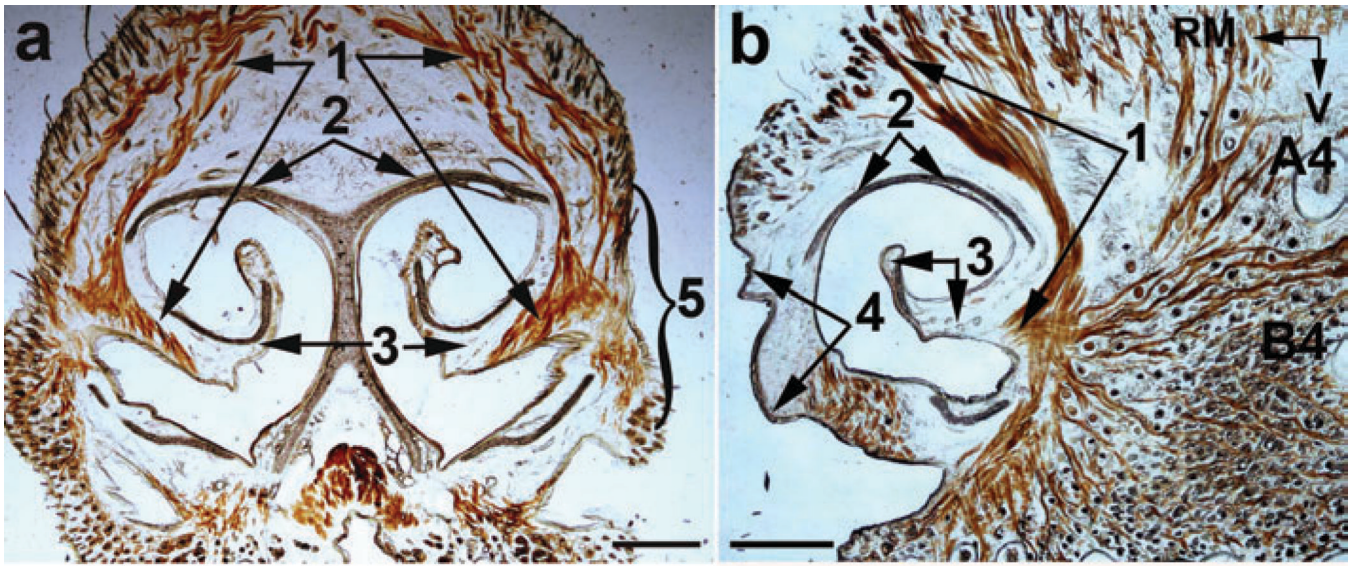

Figure 10.

Schematic image of muscles serving rhinarial motor plant. (1–6) Partes maxillares superficialis et profunda, *Pars interna profunda*, and Posterior, Pseudointrinsic, and Superficial slips, respectively, of the *Pars interna* of the *M. nasolabialis profundus*; (7) rostral slips of the *M. transversus nasi*; (8) tendon of the *M. dilator nasi*; (9*) M. levator rhinarii*; (10) *M. depressor septi nasi*; (11) *M. depressor rhinarii*. Encircled numbers indicate muscles not shared with other motor plants.

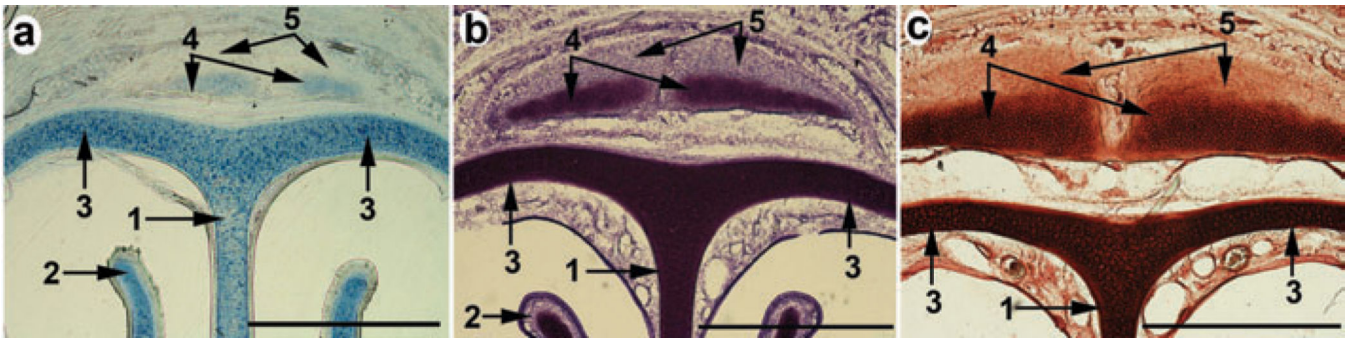

Figure 11.

Light microscopy of adult rat coronal snout slices stained with Alcian blue (a), Cresyl violet (b) and Neutral red (c). (1) Septum; (2) maxilloturbinate; (3) roof cartilage; (4) and (5) hyaline and fibrous areas, respectively, of the dorsal nasal cartilage. Scale bars = 1 mm.

Table 1

Nasofacial muscles involved in various nasofacial motor plants

Nasofacial muscles	**Rhinarial motor plant**	**Nasal olfacto-motor plant**	**Vibrissa motor plant**
M. levator Rhinarii	+	−	−
M. depressor Rhinarii	+	−	−
M. depressor septi nasi	+	+	−
Intraturbinate muscle	−	+	−
M. nasolabialis profundus, Pars anterior	−	+	−
Pars interna, Superficial slips	+	+	−
Pars interna profunda	+	+	+
Pars interna, Posterior slips	+	+	+
Pars interna, Pseudointrinsic slips	+	+	+
Pars maxillaris superficialis	+	+	+
Pars maxillaris profunda	+	+	+
Pars media superior	−	−	+
Pars media inferior	−	−	+
M. dilator nasi	+	+	+
M. transversus nasi	+	+	+
M. buccinatorius, P. orbicularis oris	−	−	+
M. maxillolabialis	−	−	+
M. nasolabialis	−	−	+
Intrinsic muscles of the mystacial pad	−	−	+